Resolving the Composite Fe Kα Emission Line in the Galactic Black Hole Cygnus X-1 with Chandra

J. M. Miller[1], A. C. Fabian[2], R. Wijnands[1,4], R. A. Remillard[1], P. Wojdowski[1], N. S. Schulz[1], T. Di Matteo[3], H. L. Marshall[1], C. R. Canizares[1], D. Pooley[1], W. H. G. Lewin[1]

Subject headings: Black hole physics – relativity – stars: binaries (Cygnus X-1) – physical data and processes: accretion disks – X-rays: stars

ABSTRACT

We observed the Galactic black hole Cygnus X-1 with the *Chandra* High Energy Transmission Grating Spectrometer for 30 kiloseconds on 2001 January 4. The source was in an intermediate state, with a flux that was approximately twice that commonly observed in its persistent low/hard state. Our best-fit model for the X-ray spectrum includes narrow Gaussian emission line (E= 6.415 ± 0.007 keV, FWHM= 80^{+28}_{-19} eV, W= 16^{+3}_{-2} eV) and broad line (E=$5.82^{+0.06}_{-0.07}$ keV, FWHM= $1.9^{+0.5}_{-0.3}$ keV, W= 140^{+70}_{-40} eV) components, and a smeared edge at 7.3 ± 0.2 keV ($\tau \sim 1.0$). The broad line profile is not as strongly skewed as those observed in some Seyfert galaxies. We interpret these features in terms of an accretion disk with irradiation of the inner disk producing a broad Fe Kα emission line and edge, and irradiation of the outer disk producing a narrow Fe Kα emission line. The broad line is likely shaped predominantly by Doppler shifts and gravitational effects, and to a lesser degree by Compton scattering due to reflection. We discuss the underlying continuum X-ray spectrum and these line features in the context of diagnosing the accretion flow geometry in Cygnus X-1 and other Galactic black holes.

[1]Center for Space Research and Department of Physics, Massachusetts Institute of Technology, Cambridge, MA 02139–4307; jmm@space.mit.edu

[2]Institute of Astronomy, University of Cambridge, Madingley Road, Cambridge CB3 OHA, UK

[3]Max-Planck-Institut fur Astrophysik, Karl-Schwarzschild-Str. 1, Postfach 1317, D85741 Garching, DE

[4]*Chandra Fellow*

1. Introduction

Cygnus X-1 was the first object to be classified as an X-ray binary system, and also the first to be recognized as a black hole, via optical radial velocity measurements (Webster & Murdin, 1971; Bolton, 1972). Correlated X-ray and radio intensity variations led to the identification of "X-ray states" — periods of high X-ray intensity and spectral softness, or low X-ray intensity and spectral hardness — in Cygnus X-1 (Tananbaum et al. 1972). Since then, states have become an essential part of how Galactic black holes are discussed and understood (for reviews, see Tanaka & Lewin 1995 and Done 2001; see also Homan et al. 2001). Cygnus X-1 has been active in X-rays since its discovery, and presently is the only known persistent Galactic black hole system with a high mass companion (an O9.7 Iab supergiant; Gies et al. 1982, 1986). The black hole mass is dynamically constrained to a lower limit of $M_{BH} \geq 9.5\ M_{\odot}$ (Paczyński 1974); Herrero et al. (1995) suggest that the most probable mass is $M_{BH} \geq 10.1\ M_{\odot}$.

The bright, persistent nature of Cygnus X-1, its constrained inclination ($i \simeq 35°$, Gies & Bolton 1986), modest distance (2.5 kpc, Bregman et al. 1973), and state transitions have made it a favorite source for observers and theorists. In particular, it is a testbed for models aiming to describe links between states and accretion flow geometries, and how these are related to the mass accretion rate ($\dot{m}$). In general, "high/soft" states are associated with high $\dot{m}$, and "low/hard" states are associated with low $\dot{m}$. State identifications usually also rely upon fast X-ray variability analysis.

A variety of models connecting states and the accretion geometry have performed well, but two show particular promise while making very different predictions. Esin et al. (1998) have described the behavior of Cygnus X-1 in terms of an advection-dominated accretion flow (ADAF). This model predicts that when $\dot{m}$ is relatively high, the disk may extend to the marginally stable orbit (the high/soft state). When $\dot{m}$ is lower, the disk is recessed, and the inner region is a hot, quasi-spherical, optically-thin ADAF. In contrast, Young et al. (2001) have described the behavior of Cygnus X-1 in terms of a disk which always extends to the marginally stable orbit but with a changing surface ionization that determines the X-ray state.

Fe Kα emission lines may trace bulk velocities, temperatures, and even strong gravitational effects. Therefore, such lines may serve as tools for placing observational constraints on accretion flow models. In some Seyfert galaxies, characteristic broad (sometimes double-peaked) Fe Kα emission lines have demonstrated the presence of an accretion disk down to the innermost stable circular orbit around the central black hole (see, e.g. Weaver, Gelbord, & Yaqoob 2001). In Galactic black holes, line profiles are often less distinct; among these systems, the lines observed in Cygnus X-1 are among the

strongest. Barr, White, and Page (1985) discovered the broad Fe Kα line (E=6.2 keV, FWHM=1.2 keV, W=120 eV) in an *EXOSAT* spectrum of Cygnus X-1. This measured centroid energy was slightly lower than the neutral value of 6.40 keV (Kaastra & Mewe 1993). Because such features are broad and relatively weak compared to lines in Seyfert galaxies, one might worry that the profiles are artifacts of poor continuum models or poor instrumental response. However, an Fe Kα line has been required to obtain statistically acceptable fits to spectra observed from Cygnus X-1 with a number of instruments, and for a variety of continuum models and source luminosities (for recent *ASCA* results, see Ebisawa et al. 1996 and Cui et al. 1998; for *BeppoSAX* results, see Di Salvo et al. 2001 and Frontera et al. 2001).

In 2000 November, Cygnus X-1 entered a high-intensity, spectrally-soft state (see, e. g., Cui, Feng, & Ertmer 2002; Pottschmidt et al. 2002). Although short high/soft states are often seen in this source, extended high/soft states are rare, previously occurring in 1980 (Ogawara et al. 1982) and 1996 (Cui 1996). The *Chandra* High Energy Transmission Grating Spectrometer (HETGS; Canizares et al. 2002, in prep.) is uniquely suited to resolving structure within broad Fe Kα lines. To test models for how accretion geometries change with source intensity (and therefore $\dot{m}$), we requested a *Chandra* observation of Cygnus X-1 to obtain a high-resolution spectrum in the Fe Kα line region during this high intensity state. We were granted a Director's Discretionary Time observation for this purpose and present results from that observation here.

Section 2 describes the instrumental configuration we used to observe Cygnus X-1. Section 3 details the models we used to fit the spectrum; the fit results are presented in Section 4. We discuss the implications of our fits for accretion flow models and compare our results on Cygnus X-1 to other Galactic black holes in Section 4. Finally, we summarize the main points of our work in Section 5. Future work will focus on the rich line spectrum below 2 keV, which has been noted in related work (Miller et al. 2001a, 2001b; see also Schulz et al. 2001, Marshall et al. 2001a), and modeling the broad-band X-ray spectrum with a variety of reflection models via simultaneous *RXTE* observations. Preliminary results from fits with the "constant-density ionized disk model" (Ross, Fabian, & Young 1999; hereafter RFY) to the 0.65-100 keV spectrum indicate an ionized accretion disk: $\log(\xi) = 3.0 - 3.5$ erg cm s^{-1}, (where $\xi = L_X/nR^2$, ξ is the ionization parameter, L_X is the X-ray luminosity, n is the hydrogen number density, and R is radius). We also find that 40-50% of the observed X-ray flux may be reflected from the accretion disk.

2. Observation and Instrumental Configuration

We observed Cygnus X-1 on 2001 January 4, from 06:03:47 to 14:49:20 (UT) – a total of 32.1 ks. Near the time of our observation, the source was flaring to some of the highest intensity levels since the 1996 "high/soft" state (see Figure 1). We identify the source state we observed as an "intermediate" state (see Section 4.1). The observatory was still slewing onto the source during the first 0.9 ks of this observation; this time span in not included for spectral analysis. A 0.5 ks dip in the X-ray lightcurve occurs 25.7 ks into this observation; during this time the count-rate drops to approximately half of the mean rate (such dips are common in Cygnus X-1; see Bałucińska-Church et al. 2000). We do not include data from within the dip for this analysis; the characteristics of the dip will be reported in a separate paper. The remaining 30.7 ks was selected for analysis. Based on the ephemeris of La Sala et al. (1998), this observation spanned a binary phase of $\phi = 0.76 - 0.82$ in the 5.6-day orbital period (with the black hole moving away from us; for a second recent ephemeris, see Brocksopp et al. 1999).

We used the HETGS to disperse the incident X-ray flux, which was read-out by the Advanced CCD Imaging Spectrometer (ACIS) spectroscopic array (ACIS-S) in continuous-clocking (CC) mode. This step was taken to reduce photon pile-up in the dispersed spectrum: the frametime in CC mode is about 2.8 ms, far less than the nominal 3.2 s in standard modes. Approximately half of the incident photons are not dispersed by the HETGS. We prevented these zeroth-order photons from being read-out with a 100-column blocking filter on the ACIS-S3 CCD. This step was taken to avoid possible telemetry saturation and dropped CCD frames. The aimpoint was moved +4 mm in the Z-direction (away from the read-out nodes) to prevent possible radiation damage to the nominal aimpoint. A Y-coordinate translation of −80 arcseconds was used to place as much of the dispersed spectrum on the ACIS-S3 CCD as possible.

At the time we conducted our analysis, the standard CIAO processing tools were unable to handle data taken in this mode. We have developed a robust set of custom processing routines. This processing method is described in detail in a paper reporting results from a *Chandra* HETGS observation of the Rapid Burster in outburst (Marshall et al. 2001b). All aspects of how the spectral grating orders and background were selected and how the data were corrected for the instrument response are as those previously reported. The only important difference between that observation and our observation of Cygnus X-1 is that the zeroth-order was blocked. The location of the zeroth order is needed to determine event wavelengths, which are a function of the dispersion distance. Without a precise measure of the location of the zeroth order, we instead use a different method to establish this relationship. We examined the locations of the neutral Si absorption edges

(due to the Si-based CCDs) in opposite grating orders. In raw counts spectra, we were able to determine the zeroth order position by iterating its location until the Si edges appeared at the same wavelength in every order. This position was fine-tuned by fitting the most prominent absorption lines in opposite grating orders and requiring that the centroid wavelengths agree to within 0.05% uncertainty (0.05% is the uncertainty in the official HETGS wavelength calibration; Canizares et al. 2002, in prep.). We are confident that our wavelength calibration is equivalent to that for standard observing modes.

We estimate that photon pile-up in our observation is negligible. Marshall et al. (2001a) report that systematic flux errors across the HETGS band are likely less than 5% in this mode. Future observations in this mode will enable better calibration and will likely make significant improvements. We find a "jump" at 2.05 keV previously seen in the spectra of bright sources observed with *Chandra* (e.g. Miller et al. 2001c; Patel et al. 2001, Juett et al. 2002). We regard this as an instrumental effect and fit it with an inverse edge ("τ"$= -0.176$). We also make note of two single-bin features near 1.85 keV (6.7 $\AA$), which are also instrumental artifacts.

3. Analysis

We considered the four first-order dispersed spectra for this analysis: the two High Energy Grating (HEG) and the two Medium Energy Grating (MEG) spectra on opposite sides of the zeroth order (hereafter, the +1 and −1 orders). An examination of these spectra revealed that the HEG +1 and MEG −1 orders are less affected by the spectrum dithering off the CCD array and relative CCD gain differences than their counterparts (due to the Z-coordinate translation). In characterizing the broad band spectrum, we therefore considered only these grating orders, with 5% systematic flux errors added in quadrature. We exclude data affected by chip gaps. Within these narrow energy ranges we included data from the HEG −1 and MEG +1 orders, normalized to the continuum level in the HEG +1 and MEG −1 orders.

Although we examined the spectrum at energies as low as 0.5 keV to understand how our absorption model fit the photoelectric oxygen absorption edge from the inter-stellar medium (ISM, see below), the MEG −1 spectrum is poorly detected below 0.65 keV. Therefore, we only fit the MEG −1 spectrum at energies above 0.65 keV. For the same reason, we only considered energies above 1.0 keV in fitting the HEG +1 spectrum. At 2.4 keV, the MEG −1 order has a chip gap, and above this energy the HEG has a higher effective area; we only consider the MEG spectra for energies below 2.4 keV. The effective upper-limit to the sensitivity of the HEG is 10.0 keV; our fits to the HEG +1 extended to

this energy.

The spectra were fit using XSPEC version 11.1.0 (Arnaud 1996). The MEG −1 and HEG +1 spectra were fit jointly, allowing an overall normalization constant to float between them (generally, the constant indicated that the normalization agreed to within 2% or better). Systematic errors were added to the flux values using the FTOOL "grppha." Significances quoted in this paper were calculated using the F-statistic with the "ftest" task within XSPEC.

All spectral models were multiplied by a model for photoelectric absorption in the ISM, with variable elemental abundances. Local fits to the absorption edges agree with the absorption model reported in a previous *Chandra* observation of Cygnus X-1 by Schulz et al. (2001). We used the "vphabs" model in all fits with the abundances adjusted to agree with Schulz et al. (2001), with the minor distinction that we used the Verner et al. (1993) cross-sections to fit the Fe L3 edge, and that we found no evidence for the Fe L1 edge. Several components of this model should be noted: the neutral hydrogen column density is 6.21×10^{21} cm^{-2}, oxygen is 7% under-abundant (relative to solar) and a better fit is obtained for an edge at 0.536 keV rather than the predicted 0.532 keV, iron is 25% under-abundant, neon is 11% over-abundant, and all other edges are consistent with solar values (relative to the abundances stated by Morrison & McCammon 1983; $A_{Fe}/A_H \simeq 3.3 \times 10^{-5}$) and expected wavelengths. These absorption values were not allowed to vary in fits to the 0.65–10.0 keV spectrum.

A wide variety of models have been used to fit the X-ray spectrum of Cygnus X-1. These range from models which attempt to describe Compton-upscattering of seed photons in a corona, to more phenomenological models. Often, these cannot be distinguished on the basis of a goodness-of-fit statistic (see, e.g., Nowak, Wilms, & Dove 2002). As an example of the former, we attempted to fit the observed 0.65-10.0 keV spectrum with the "compTT" model (Titarchuk et al. 1994). We also fit the spectrum with a model consisting of the multicolor disk blackbody (hereafter, MCD; Mitsuda et al. 1984) model and a power-law. This additive model is commonly a good fit to Galactic black hole spectra, and provides a standard for comparison to other sources. The breadth and strength of Fe Kα line and K edge features are sufficient to affect fits to the underlying continuum, and so we have analyzed the continuum and Fe Kα line region jointly.

4. Results

4.1. The Continuum Spectrum

In Figure 2, we show the results of fitting an MCD plus power-law model to the spectra (Model 1 in Table 1, but without a narrow Gaussian line component). A soft, thermal component is not required in some low/hard state spectra observed with other instruments. However, in this observation such a component is strongly required. In Panels A and B of Figure 2, structure is apparent in the Fe Kα line region – most notably a very narrow emission line.

Fits with the compTT model were not statistically acceptable. The seed photon temperature and electron temperature of the Compton-upscattering corona could not be constrained (errors on these parameters were several times larger than the values measured). Fitting only this model, $\chi^2/\nu > 8$ (where ν is the number of degrees of freedom in the fit). Fitting an MCD component simultaneously with compTT yielded a better but still unacceptable fit ($\chi^2/\nu > 3$). Moreover, the data/model ratio shows the same structure in the Fe Kα line region that is seen in Panel B of Figure 2. Hereafter, we restrict our discussion to MCD plus power-law models. We note that compTT may still be a good description of spectra from Cygnus X-1 in different states.

In Table 1, we list the parameters obtained by fitting a series of MCD plus power-law models with different local models for the Fe Kα line region. Model 1 includes a narrow Gaussian to fit the narrow line evident in Panel B of Figure 2 (see also Figures 3 and 4). Model 2 adds a smeared edge component ("smedge," Ebisawa et al. 1994). Model 3 adds a Gaussian to Model 2 to fit a broad emission line. Model 4 adds the "diskline" model (Fabian et al. 1989) to Model 2 instead of a Gaussian. The diskline model explicitly takes into account the Doppler and general relativistic shifts expected for a line produced via the irradiation of an accretion disk near to a black hole.

These models yield apparently poor fits: $\chi^2/\nu \simeq 1.8$. This is due to the fact that we have not fit a model for the complex absorption spectrum below 2 keV (Miller et al. 2001a, 2001b; Schulz et al. 2001; Marshall et al. 2001b). We include this energy range because it is critical for accurately characterizing the overall continuum shape. Fitting the same models to the spectrum in the 1.8–10.0 keV band (chosen to include the instrumental jump at 2.05 keV), statistically acceptable fits are obtained: $\chi^2/\nu \simeq$0.85–1.15. Thus, we believe that the fits obtained on the 0.65–10.0 keV band are meaningful.

The peak color temperatures of the inner accretion disk measured via the MCD model ($kT = 0.236 \pm 0.002$ keV with Model 3) are above those which have been measured in the low/hard state (e.g. Ebisawa et al. 1996), and below those measured in the high/soft state (e.g. Cui et al. 1998). The power-law indices we measure ($\Gamma = 1.84 \pm 0.01$ with

Model 3) are similarly intermediate. Assuming a distance of 2.5 kpc to Cygnus X-1, we measure $L_X = 1.03 \pm 0.02 \times 10^{37}$ ergs/s (0.5-10.0 keV) with Model 3. This luminosity is approximately twice that commonly measured in low/hard state, but not as high as the luminosities observed during the high/soft states observed previously in 1980 and 1996. Indeed, Belloni et al. (1996) identify the activity in 1996 as an "intermediate" state based partially on a blackbody temperature of $kT = 0.36 \pm 0.01$ keV and a power-law index of $\Gamma = 2.15 \pm 0.02$ (the latter being intermediate between canonical low/hard and high/soft state values). As the spectrum and luminosity we have observed with *Chandra* are between typical low/hard and high/soft states values, we characterize this as an "intermediate" state. However we note that it is a different kind of intermediate state than described by Belloni et al. (1996) in that it is spectrally harder.

If the distance towards a source and its inclination are known, the MCD model provides a measure of the innermost extent of the accretion disk. Assuming a distance of 2.5 kpc and $i = 35°$, and $M_{BH} = 10\ M_\odot$, our fits indicate the inner disk may extend very close to the marginally stable circular orbit: $R_{in} = 8.7 \pm 0.2\ R_g$ (where $R_g = GM_{BH}/c^2$) via Model 3. As R_{in} scales directly with the source distance in the MCD model, if the distance to Cygnus X-1 is uncertain at the 25% level the inner disk extent should have approximately the same fractional uncertainty. Errors in the inclination are less important, but non-negligible for intermediate values. Therefore, we regard the inner disk extent measured via the MCD model to be consistent with the marginally stable circular orbit for a Schwarzschild black hole (6 R_g) for a small range of masses near 10 $M_\odot$.

Shimura and Takahara (1995) have proposed corrections to the MCD model to account for Comptonization of the inner disk flux. They suggest that $kT_{in,corrected} = kT_{MCD}/f$ and $R_{in,corrected} = f^2 \times R_{in,MCD}$; $f = 1.7$ is suggested as appropriate for Galactic black holes. If such a correction is valid, the inner disk may be somewhat larger than the marginally stable orbit in the intermediate state. Merloni, Fabian, & Ross (2000) have noted that the MCD model may systematically underestimate the inner disk extent and imply a changing inner disk radius at low $\dot{m}$, but yield acceptable measures at relatively high $\dot{m}$. As we have observed Cygnus X-1 at a soft X-ray luminosity approximately twice as high as its persistent luminosity, the MCD model may give acceptable estimates of the inner disk extent. In principle, the Fe Kα line can serve as a check on the inner accretion disk extent. The FWHM of the broad Fe Kα line we discuss below is consistent with Keplerian velocities expected if the inner accretion disk extends near to the marginally stable circular orbit, suggesting $f \simeq 1.0$ may be more appropriate in this state than $f = 1.7$.

4.2. The Fe $K\alpha$ Line Region

The complexity of the Fe Kα line region can be seen clearly via two methods. In Figure 3, the fit to the spectrum in the Fe Kα line region with Model 3 is shown in detail. In Figure 4, we show the data/model ratio for a model which does not include components to fit the Fe Kα line region, following the procedure that Iwasawa et al. (1996) used to represent the Fe Kα line in MCG –6–30–15.

Relative to a model with no component to fit the narrow emission line, the narrow Gaussian included in Model 1 is significant at the 6.0σ level of confidence in the 0.65–10.0 keV band and above 8.0σ in the 1.8–10.0 keV band. The line measured via Model 1 is centered at 6.415 ± 0.007 keV; this value is fixed in Models 3 and 4. If this line were due mostly to Fe I, this centroid energy would represent a blue-shift of 560 ± 330 km/s. The FWHM width of the line varies slightly depending on the underlying continuum model, but is easily resolved with the HEG. Via Model 3, we measure a FWHM of 59^{+24}_{-14} eV, or 2800^{+1100}_{-660} km/s; a FWHM of 80^{+28}_{-19} eV, or 3700^{+1300}_{-890} km/s is obtained via Model 1. The equivalent width of the line also depends slightly on the underlying continuum: via Model 1 we obtain W$= 22 \pm 4$ eV; Model 3 gives W$= 16^{+3}_{-2}$ eV.

The apparent blue-shift of the narrow line from Fe I at 6.401 keV may be explained in terms of a line mostly comprised of Fe II, and partially comprised of species below Fe IX (Kaastra & Mewe 1993). Similarly, the measured FHWM of the line can be partially explained in these terms. Alternatively, one may want to argue that the line is due mostly to Fe I, and that the blue-shift and FWHM velocities are physical. However, the blue-shift is less than the terminal velocity expected for a type-O stellar wind (1500 km/s; Castor, Abbot, & Klein 1975); it is reasonable to assume that a neutral part of the wind must be relatively far from the ionizing flux originating near the black hole, and therefore close to terminal velocity. Moreover, the blue shift is far less than the jet velocity ($v/c > 0.6$) inferred from a spectral model by Stirling et al. (2001) in the low/hard state of Cygnus X-1. It is more likely that the shift and FWHM are partially explained by a line produced by a few moderately ionized species at a point more internal to the system.

The measured strength of the narrow Fe K$_\alpha$ line is consistent with *ASCA* measurements of 10–30 eV by Ebisawa et al. (1996), made during low/hard states. Assuming solar Fe abundances, Ebisawa et al. estimated that the maximum narrow line equivalent width expected due to excitation of the companion star surface and wind is ≤ 11.1 eV. On this basis, Ebisawa et al. suggested that the narrow line was most likely due to the irradiation of the outer accretion disk. This scenario is consistent with the reflection geometry many authors have claimed in Cygnus X-1 (see, e.g., Gierłinski et al. 1997, 1999). Schulz et al. (2001) measured Fe to be 25% under-abundant in Cygnus X-1 ($A_{Fe}/A_H \simeq 3.3 \times 10^{-5}$; as

per Morrison & McCammon 1983); if this under-abundance is intrinsic to the system, the maximum expected line equivalent width due to excitation of the companion wind and surface is ≤ 8.3 eV. We conclude that approximately half of the strength of the line we observe must be produced via other means. We conclude that the irradiation of the cool outer accretion disk is likely to account for the extra line strength.

Upper-limits on the strength of an Fe Kβ emission line at 7.06 keV (assuming the same FWHM measured for the Kα line) are not very constraining. The broad emission line and smeared edge both contribute at 7.06 keV, and these components may obscure a weak Kβ line. The Kβ/Kα line ratio is consistent with the expected value of 0.13.

We regard the broad Gaussian plus smeared edge of Model 3, and diskline plus smeared edge in Model 4, as approximations to a self-consistent treatment of the Doppler and GR effects expected near to a black hole, and to broadening effects expected if reflection is important. The smeared edge in Models 2, 3, and 4 has a fixed width of 7.0 keV, as observed in other Galactic black holes (see, e.g., Sobczak et al. 1999). We fix the smearing width because the energy range of Chandra is not sufficient to constrain this parameter. The edge energy is fixed at 7.11 keV (for Fe I) in Model 2, but is allowed to vary in Models 3 and 4 (edge energies of 7.3 ± 0.1 keV and 7.2 ± 0.1 keV are measured, respectively). In Model 3, the maximum optical depth is $\tau = 1.0 \pm 0.2$. The addition of the smeared edge component in Model 2 is significant at the 5.2σ level of confidence in the 0.65–10.0 keV band, and at 7.2σ in the 1.80–10.0 keV band.

The addition of the diskline component Model 4 is only significant the 3.1σ level of confidence in the 0.65–10.0 keV band, but is significant at more than 8.0σ in the 1.80–10.0 keV band. The centroid energy measured is 5.85 ± 0.06 keV. The inclination was moderately-well constrained: $i = 40^\circ \pm 10^\circ$. We note that this measurement is broadly consistent with optical measurements of the inclination ($i = 35^\circ$, Gies & Bolton 1986, Herrero et al. 1995). Assuming an accretion disk emissivity profile with an outer line excitation radius of 1000 R_g, the inner disk extent measured by the inner disk model is $R_{in} = 7^{+6}_{-1}\ R_g$. This value is consistent with the values we measured with the MCD model and consistent with the marginally stable orbit around the black hole. Note that this model does not assume a black hole mass, or a distance to the source, which are necessary to derive inner disk radii in units of R_g with the MCD model. Fits with the "Laor" model (Laor 1991) for a line produced at the inner accretion disk around a Kerr black hole did not require an inner disk edge inside the marginally stable circular orbit for a Schwarzschild black hole.

Model 3 provides a better fit to the data, using a simple Gaussian to model (see Figure 3) a broad Fe Kα emission line. This Gaussian component is significant at the 4.3σ level of

confidence in the 0.65–10.0 keV band, and at more than 8.0σ in the 1.80–10.0 keV band. The measured Gaussian centroid energy is $5.82^{+0.06}_{-0.07}$ keV and the FWHM is very broad: $1.9^{+0.5}_{-0.3}$ keV. The line is relatively strong: W= 140^{+70}_{-40} eV, but consistent with many previous measurements of this feature. As strong Doppler shifts and gravitational red-shifts may be expected from the inner accretion disk, it is likely that this line is produced via irradiation of the inner accretion disk.

We have addressed the significance of the broad Fe Kα emission line statistically, but an additional note is merited. One would expect that if an instrumental response error falsely creates a broad line profile, that it should be seen in all observations of bright sources made with *Chandra*. A review of the literature reveals that this is not the case. Moreover, *Chandra* observations of the Galactic black holes XTE J1550 −564 at a flux of 0.6 Crab using our instrument mode (Miller et al. 2001d), and GRS 1915+105 at a flux of 0.4 Crab using a standard instrument mode (Lee et al. 2001), do *not* reveal clear evidence for narrow or broad Fe Kα emission lines. These facts give us additional confidence that the line we have observed is intrinsic to Cygnus X-1, and not due to the instrumental response.

The FWHM of the broad line implies Doppler shifts which are a significant fraction of c and consistent with Keplerian velocities near the marginally stable orbit around a Schwarzschild black hole. As noted above, gravitational effects may also shape the line profile. However, other effects may be important. As Fe Kα line photons produced through disk reflection propagate through the disk and/or an ionized disk skin, they may undergo Compton scattering. Here, we estimate the degree of line broadening due to this process. The broadening per scattering is given by: $\frac{\Delta \mathrm{E}}{\mathrm{E}} = (\frac{2kT}{m_e c^2})^{0.5}$. The inner accretion disk color temperature we have measured with the MCD model is < 0.3 keV. RFY find that an thin ionized atmosphere above the disk in Cygnus X-1 may have a temperature of approximately $kT \sim 1.3$ keV. These values give a broadening per scatter of 3% and 7%, respectively. For an Fe Kα line with a FWHM similar to that of the narrow line we observe, approximately 50 scattering events in a $kT \sim 1.3$ keV disk skin are required to reproduce the full width of the broad line we observe. For $\xi = 10^4$ (slightly above what we observe in Cygnus X-1 in this state; see Section 1), RFY find that Fe XXV has a maximum ion fraction for $\tau_{Thomson} \sim 5$, suggesting as many as ~ 25 scattering events. A hot coronal volume (with $kT \sim 30$ keV, or higher) is not expected to contribute to line broadening significantly as such volumes are likely to be optically thin. As the FWHM of the line we observe corresponds to $\Delta \mathrm{E}/\mathrm{E} \sim 0.3$, for a range of disk temperatures and ionized skin temperatures Compton scattering is likely to be a relatively small but non-negligible broadening mechanism compared to Doppler shifts and gravitational effects.

5. Discussion

A combination of an elevated source intensity, the resolution of the *Chandra* HETGS, and a ∼30 ks exposure have allowed us to resolve the Fe Kα line region in the X-ray spectrum of Cygnus X-1 for the first time. We clearly detect a narrow Fe Kα emission line, a broad Fe Kα emission line, and a smeared Fe K edge (see Figures 3 and 4).

These features can be explained in terms of an accretion disk illuminated by a source of hard X-rays, with the broad line and edge due to irradiation of the inner accretion disk, and the narrow line due to irradiation of the outer accretion disk. This scenario is predicted by reflection models for AGNs and Galactic black holes (see, e.g., George & Fabian 1991; Ross, Fabian, & Young 1999, Nayakshin & Dove 2001). The broad components are consistent with previous observations of Cygnus X-1 (see Ebisawa et al. 1996, Cui et al. 1998, and Frontera et al. 2001, among others). The narrow line is consistent with upper-limits from *ASCA* (Ebisawa et al. 1996).

The broad emission line is broader than that reported in most previous observations of Cygnus X-1 and other Galactic black holes and may be slightly red-shifted. The broad line is not clearly double-peaked or skewed like those observed in AGNs with *ASCA* (for a review, see Weaver, Gelbord, & Yaqoob 2001; Yaqoob et al. 2002), or in an *XMM-Newton* observation of MCG –6–30–15 by Wilms et al. (2001). The broad line has a centroid energy of E= $5.82^{+0.06}_{-0.07}$ keV, which differs significantly from Fe I at 6.40 keV. The line profile we have observed may be regarded as evidence for a line which is shifted and/or partially shaped by strong gravitational effects.

Previous observations of Cygnus X-1 with the *Chandra* HETGS have not clearly revealed similar structure in the Fe Kα line region. Schulz et al. (2001) observed this source at a similar flux level for 15 ks (half of the exposure time we report on), though with an observing mode less suited to this work and suffering heavily from CCD pile-up, forcing the use of higher-order spectra with lower sensitivity. Cygnus X-1 was observed for 15 ks in the low/hard state, at a flux approximately half of the intensity we measured. Preliminary results have been reported by Marshall et al. (2001b). The low/hard state observation does not reveal a narrow emission line, but may show evidence for a weak, broad emission line and smeared edge. If the outer accretion disk is relatively more flared in the intermediate state than the low/hard state, this could explain why a narrow line is only detected in our observation. The lack of clearly detected lines in other *Chandra* observations of Cygnus X-1 may indicate that the line is variable. However, it is possible that long exposures in the future with well-suited instrument modes will reveal structure in the Fe Kα line region across a range of source intensities.

Previous observations of transient Galactic black holes have also revealed evidence for broad Fe Kα emission lines, though few are as clear as the profiles observed in Cygnus X-1. Among the sources recently observed, broad lines have been been detected in XTE J1550−564 (Sobczak et al. 2000), GRO J1655−40 (Sobczak et al. 2000, Bałucińska-Church & Church 2000), GX 339−4 (Nowak, Wilms, & Dove 2002), XTE J1748−288 (Miller et al. 2001e), V4641 Sgr (in't Zand et al. 2000), and XTE J2012+381 (Campana et al. 2001). These lines have been observed in the "very high" state and in intermediate states. In both of these states, the inner accretion disk temperature in these transient systems is relatively high: $kT = 0.7 - 1.2$ keV is common. Moreover, the inclinations of GRO J1655−40 (Greene, Bailyn, & Orosz 2001) and XTE J1550−564 (Orosz et al. 2001) are $i = 70^\circ \pm 2^\circ$ and $i = 72^\circ \pm 5^\circ$, respectively. The relatively cool inner disk we have observed in the intermediate state of Cygnus X-1 ($kT = 0.236 \pm 0.002$ keV) makes continuum flux from the disk less important in the Fe Kα line region than in transient systems. The low inclination ($i \simeq 35^\circ$) of Cygnus X-1 may also reveal irradiation of the inner disk more clearly than transient black holes with high inclinations.

The Fe Kα line provides an important diagnostic of the innermost extent of the accretion disk. The breadth of the line and edge we have observed — if produced at the inner accretion disk — require a disk which extends close to the marginally stable circular orbit. The line profile is consistent with the values of the inner disk extent we have measured with the MCD model. This finding supports the ionized disk model of Young et al. (2001) for X-ray states in Cygnus X-1 (for another discussion of ionized transition layers, also see Życki, Done, & Smith 2001). The inner disk extent in the intermediate state may be particularly incisive in evaluating the ADAF model. Esin et al. (1998) found that the disk may extend to the marginally stable orbit in the high/soft state of Cygnus X-1, but may have recessed to 200 R_g in the low/hard state. That the inner disk extent is consistent with the marginally stable orbit in this intermediate state suggests the inner disk may not recede smoothly as a function of the mass accretion rate in Cygnus X-1. In commenting on the ionized disk and ADAF models, it must be noted that within the larger set of states and behaviors observed in Cygnus X-1, this state may prove to be peculiar. Several future observations of Cygnus X-1 at high resolution are required to further evaluate these models.

6. Conclusions

The main results of this paper may be summarized as follows:

• We have resolved the Fe Kα line region into a narrow line consistent with the excitation of low ion species, and a very broad emission line and edge combination. The

lines are likely produced via the irradiation of the accretion disk, with the broad line produced at the inner accretion disk and the narrow line excited at the outer accretion disk. This is consistent with models for X-ray reflection in Galactic black holes and AGNs. The broad line shape may be determined predominantly by a combination of Doppler shifts, the gravitational field of the black hole, and also by Compton scattering in the accretion disk and/or an ionized disk skin as part of the reflection process.

• Based on the accretion disk temperature, the photon power-law index, and the X-ray flux observed, we conclude that we observed Cygnus X-1 in an intermediate state.

• In this intermediate state, the MCD model suggests that the inner accretion disk extends close to the marginally stable orbit. This finding is supported by the broad Fe Kα line and edge profiles. Thus, an inner ADAF is not required to describe this state of Cygnus X-1.

• When well-suited observational modes and long exposures are used to observe bright galactic sources, the *Chandra* HETGS is capable of resolving composite lines into components. This result holds great promise for understanding the accretion flow geometry in Galactic black holes and neutron stars via Fe Kα line diagnostics.

7. Acknowledgments

We wish to thank *Chandra* Director Harvey Tananbaum, and the *Chandra* staff for executing this observation and their help in processing the data. We thank Michael Nowak for useful discussions. RW was supported by NASA through Chandra fellowship grants PF9-10010, which is operated by the Smithsonian Astrophysical Observatory for NASA under contract NAS8–39073. HLM and NSS are supported under SAO contract SAO SV1-61010. WHGL gratefully acknowledges support from NASA. This research has made use of the data and resources obtained through the HEASARC on-line service, provided by NASA-GSFC.

REFERENCES

Arnaud, K. A., 1996, Astronomical Data Analysis Software and Systems V, eds. Jacoby G. and Barnes J., p17, ASP Conf. Series volume 101

Bałucińska-Church, M., & Church, M. J., 2000, MNRAS, 312L, 55

Bałucińska-Church, M., Church, M. J., Charles, P. A., Nagase, F., LaSala, J., & Barnard, R., 2000, MNRAS 311, 861

Barr, P., White, N. E., and Page, C. G., 1985, MNRAS 216, 65

Belloni, T., Mendez, M., van der Klis, M., Lewin, W. H. G., and van Paradijs, J., 1996, ApJ, 472, L107

Beloborodov, A. M., 1999, ApJ, 510L, 123

Bolton, C. T., 1972, Nature, 235, 271

Bregman, J., Butler, D., Kemper, E., Koski, A., Kraft, R. P., & Stone, R. P. S., 1973, ApJ, 185, L117

Brocksopp, C., et al., 1999, MNRAS, 309, 1063

Campana, S., et al., 2001, A & A, in press, astro-ph/0112485

Castor, J. I., Abbot, D. C., & Klein, R. I., 1975, ApJ, 195, 157

Cui, W., 1996, IAU Circ. 6404

Cui, W., Ebisawa, K., Dotani, T., and Kubota, A., 1998, ApJ, 493, L75

Cui, W., Feng, Y., & Ertmer, M., 2002, ApJ, 564, 77L

Di Salvo, T., Done, C., Życki, P. T., Burderi, L., and Robba, N. R., 2001, ApJ, 547, 1024

Done, C., 2001, AdSpR, 28, 255

Ebisawa, K., et al., 1994, PASJ, 46, 375

Ebisawa, K, Ueda, Y., Inoue, H., Tanaka, Y., and White, N. E., 1996, ApJ, 497, 419

Esin, A. A., Narayan, R., Cui, W., Grove, E. J., and Zhang, S. N., 1998, ApJ, 505, 854

Fabian, A. C., Rees, M. J., Stella, L., and White, N. E., 1989, MNRAS, 238, 729

Frontera, F., et al., 2001, ApJ, 546, 1027

George, I. M., & Fabian, A. C., 1991, MNRAS, 249, 352

Gierłinski, M., Zdziarski, A. A., Done, C., & Johnson, W., N., 1997, MNRAS, 288, 958

Gierłinski, M., Zdziarski, A. A., Poutanen, J., Coppi, P. S., Ebisawa, K., & Johnson, W. N., 1999, MNRAS, 309, 496

Gies, D. R., & Bolton, C. T., 1982, ApJ, 260, 240

Gies, D. R., & Bolton, C. T., 1986, ApJ 304, 371 & 389

Greene, J., Bailyn, C. D., & Orosz, J. A., 2001, ApJ, 554, 1290

Herrero, A., Kudritzki, R. P., Gabler, R., Vilchez, J. M., & Gabler, A., 1995, A & A, 297, 556

Homan, J., et al., 2001, ApJS, 132, 377

Iwasawa, K., Fabian, A.C., Young, A. J., Inoue, H., Matsumoto, C., 1999, MNRAS 306L, 19

Juett, A., et al., 2002, ApJL, subm.

Kaastra, J. S., & Mewe, R., 1993, A & AS, 97, 443

Laor, A., 1991, ApJ, 376, 90

LaSala, J., Charles, P. A., Smith, R. A. D., Bałucińska-Church, M., & Church, M. J., 1998, MNRAS, 301, 285

Marshall, H. L., Schulz, N. S., Fang, T., Cui, W., Canizares, C. R., Miller, J. M., & Lewin, W. H. G., 2001a, Proc. of "X-ray Emission from Accretion onto Black Holes," Eds. T. Yaqoob and J. Krolik, astro-ph/0111464

Marshall, H. L., et al., 2001b, AJ, 122, 21

Merloni, A., Fabian, A. C., & Ross, R. R., 2000, MNRAS, 313, 193

Miller, J. M., et al., 2001a, AAS 198.8001

Miller, J. M., et al., 2001b, in "X-ray Emission from Accretion onto Black Holes," eds. T. Yaqoob and J. H. Krolik, published electronically

Miller, J. M., Ballantyne, D. R., Fabian, A. C., and Lewin, W. H. G., 2001c, MNRAS, subm., astro-ph/0111027

Miller, J. M., et al., 2001d, MNRAS, subm., astro-ph/0103215

Miller, J. M., et al., 2001e, ApJ, 546, 1055

Mitsuda, K., et al., 1984, PASJ, 36, 741

Morrison, R., & McCammon, D., 1983, ApJ, 270, 119

Nayakshin, S., and Dove, J. B., 2001, ApJ, 560, 885

Nowak., M. A., Wilms, J., & Dove, J. B., 2002, MNRAS, in press

Ogawara, Y., et al., 1982, Nature, 295, 675

Orosz, J. A., et al., 2001, ApJ, in press, astro-ph/0112101

Paczyński, S., 1974, A & A, 34, 161

Patel, S. K., et al., 2001, ApJL, in press, astro-ph/0110182

Pottschmidt, K., et al., 2002, A & A, subm., astro-ph/0202258

Ross, R. R., Fabian, A. C., & Young, A. J., 1999, MNRAS, 306, 461

Schulz, N. S., Cui, W., Canizares, C. R., Marshall, H. L., Lee, J. C., Miller, J. M., and Lewin, W. H. G., 2001, ApJ, in press

Shimura, T., & Takahara, F., 1995, ApJ, 445, 780

Sobczak, G. J., McClintock, J. E., Remillard, R. A., Bailyn, C. D., & Orosz, J. A., 1999, ApJ 520, 776

Sobczak, G. J., et al., 2000, ApJ, 544, 993

Stirling, A. M., Spencer, R. E., de la Force, C. J., Garrett, M. A., Fender, R. P., Ogley, R. N., 2001, MNRAS, 327, 1273

Tanaka, Y., et al., 1995, Nature, 375, 659

Tanaka, Y., & Lewin, W. H. G., 1995, X-ray Binaries, ed. W. H. G. Lewin et al. (Cambridge: Cambridge Univ. Press), 126

Tananbaum, H., Gursky, H., Kellogg, E., Giacconi, R., & Jones, C., 1972, ApJ, 177L, 5

Titarchuk, L., 1994, ApJ, 434, 570

Verner, D. A., Yakovlev, D. G., Band, I. M., & Trzhaskovskaya, M. B., 1993, At. Data Nucl. Data Tables, 55, 252

Weaver, K., Gelbord, J., & Yaqoob, T., 2001, ApJ, 550, 261

Webster, B. L., & Murdin, P., 1971, Nature, 250, 183

Wilms, J., et al., 2001, MNRAS, in press, astro-ph/0110520

Yaqoob, T., Padmanabhan, U., Dotani, T., & Nandra, K., 2001, ApJ, in press, astro-ph/0112318

Young, A. J., Fabian, A. C., Ross, R. R., and Tanaka, Y., 2001, MNRAS, 325, 1045

in 't Zand, J. J., M., 2000, A & A, 357, 520

Życki, P., Done, C., & Smith, D. A., 2001, MNRAS, 326, 1380

Table 1: Models for the 0.65-10.0 keV Spectrum of Cygnus X-1

	Model 1	Model 2	Model 3	Model 4
(MCD[a])				
kT (keV)	0.240(3)	0.241(2)	0.236(2)	0.239(2)
Norm. (10^5)	2.04(8)	1.99(7)	2.14(9)	2.07(7)
R_{in} (R_g)	8.5(2)	8.4(2)	8.7(2)	8.5(2)
Flux (10^{-8} cgs)	0.36(1)	0.36(1)	0.35(1)	0.36(1)
(Power-law)				
Γ	1.789(9)	1.78(1)	1.84(2)	1.80(1)
Norm.	2.009(9)	1.98(2)	2.09(2)	2.03(2)
Flux (10^{-8} cgs)	1.040(5)	1.014(8)	1.04(1)	1.03(1)
L_X^a (10^{37} cgs)	1.05(2)	1.03(2)	1.03(2)	1.04(2)
(Narrow Line)				
E (keV)	6.415(7)	$6.415^{+0.007}_{-0.003}$	6.415	6.415
σ (eV)	34^{+12}_{-8}	36^{+6}_{-11}	25^{+10}_{-6}	30(6)
W (eV)	22(4)	20(4)	16^{+3}_{-2}	22(3)
Norm. (10^{-3})	1.6(3)	$1.6^{+0.2}_{-0.4}$	1.2(3)	1.6(2)
Flux (10^{-11} cgs)	1.7(3)	$1.7^{+0.2}_{-0.4}$	1.2(3)	1.7(2)
(Broad Line)	–	–	(Gaussian)	(Diskline[c])
E (keV)	–	–	$5.82^{+0.06}_{-0.07}$	5.85(6)
σ (keV)	–	–	$0.8^{+0.2}_{-0.1}$	–
W (eV)	–	–	140^{+70}_{-40}	60^{+12}_{-6}
Norm. (10^{-3} cgs)	–	–	12^{+6}_{-3}	$4.5^{+0.9}_{-0.4}$
Flux (10^{-11} cgs)	–	–	12^{+6}_{-3}	$4.0^{+0.8}_{0.4}$
R_{in} (R_g)	–	–	–	7^{+6}_{-1}
i (degrees)	–	–	–	40(10)
(Smeared Edge)				
E (keV)	–	7.11	7.3(2)	7.2(1)
τ	–	1.5(3)	1.0(2)	1.2(2)
(1.80–10.0 keV)				
χ^2	1176.94	1130.69	1104.20	1114.45
d.o.f.	1293	1292	1289	1287
$P^b_{F-statistic}$	8.5×10^{-21} ($> 8.0\sigma$)	6.2×10^{-13} (7.2σ)	2.6×10^{-19} ($> 8.0\sigma$)	5.0×10^{-18} ($> 8.0\sigma$)
(0.65-10.0 keV)				
χ^2	6576.86	6527.52	6482.62	6493.93
d.o.f.	3614	3613	3610	3608
$P^b_{F-statistic}$	2.0×10^{-9} (6.0σ)	1.8×10^{-7} (5.2σ)	1.6×10^{-5} (4.3σ)	2.3×10^{-3} (3.1σ)

Note. — Errors on the MCD and power-law components are 90% confidence errors, and errors on line parameters are 1σ errors. Where errors are symmetric, they are indicated in parentheses. Single-digit errors reflect the error in the last significant digit. Where errors are not quoted, the parameter was fixed at the value indicated. The ISM absorption model of Schulz et al. (2001) was used in fitting the spectra. [a] We assume $i = 35°$ and $d = 2.5$ kpc (see text for references). [b] P is the F-statistic probability that the improvement in the χ^2 fitting statistic is due to random fluctuations. For Model 1, P is quoted for the addition of the Gaussian model for the narrow Fe Kα line to the same model with no lines. For Model 2, P relates to the addition of the smeared Fe K edge model "smedge" versus Model 1. For Models 3 and 4, P is quoted for the addition of Gaussian and "diskline" models (respectively) for the broad Fe Kα line component, relative to Model 2. P was calculated using the "ftest" task within XSPEC version 11.1.0 (Arnaud 1996). Underneath each P value, the significance of the feature is indicated in parentheses. The apparently poor fits in the 0.65–10.0 keV band ($\chi^2/\nu \sim 1.80$) are due to complex line spectrum below 2 keV. We also quote the results of fitting these models on the 1.8–10.0 keV range, which avoids much of the absorption but allows the instrumental feature at 2.0 keV to be constrained. [c] An accretion disk emissivity profile was assumed for the diskline model.

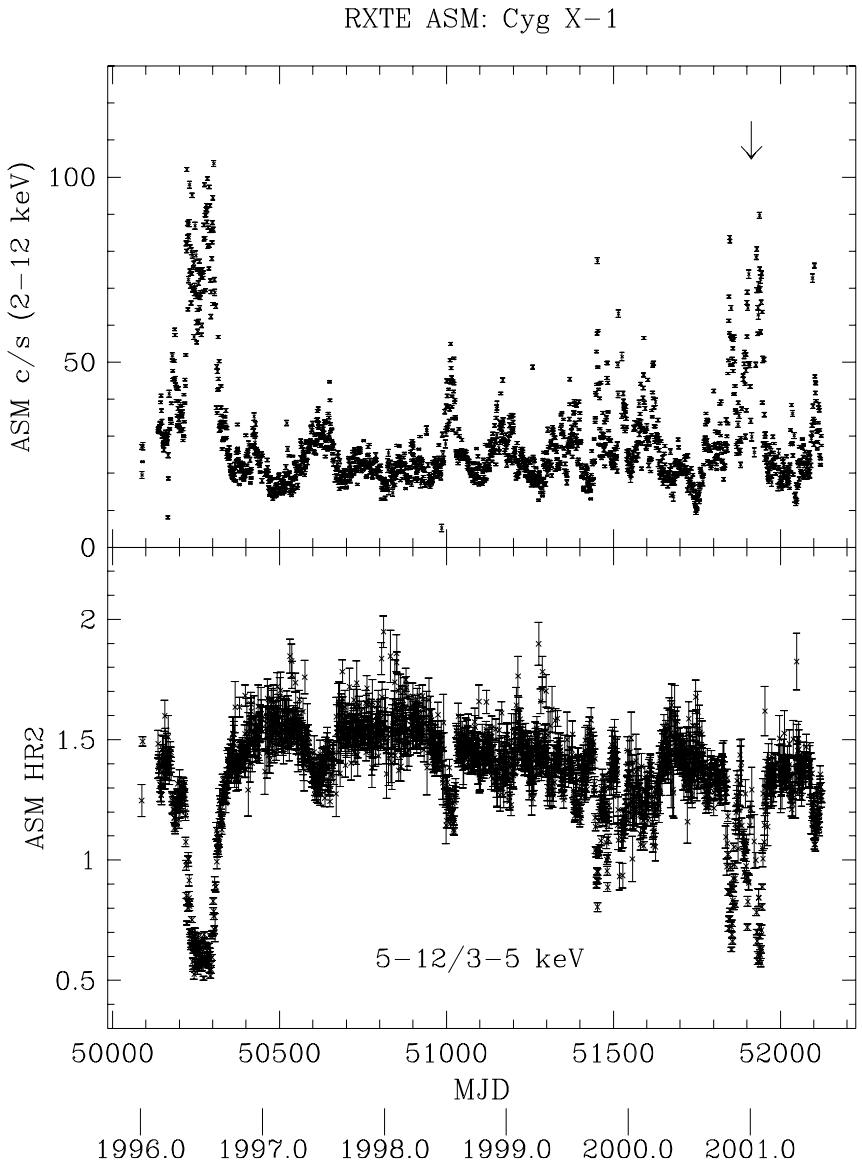

Fig. 1.— The *RXTE*/ASM lightcurve and (5-12 keV)/(3-5 keV) hardness ratio for Cygnus X-1. The curves shown here span a time interval from the start of the mission until shortly after our *Chandra* observation on 2001 January 4 (indicated by the arrow in the lightcurve). On this day, Cygnus X-1 was observed at 34 c/s with the ASM. The source was the midst of the softest, highest-intensity period observed until that point since the 1996 high/soft state.

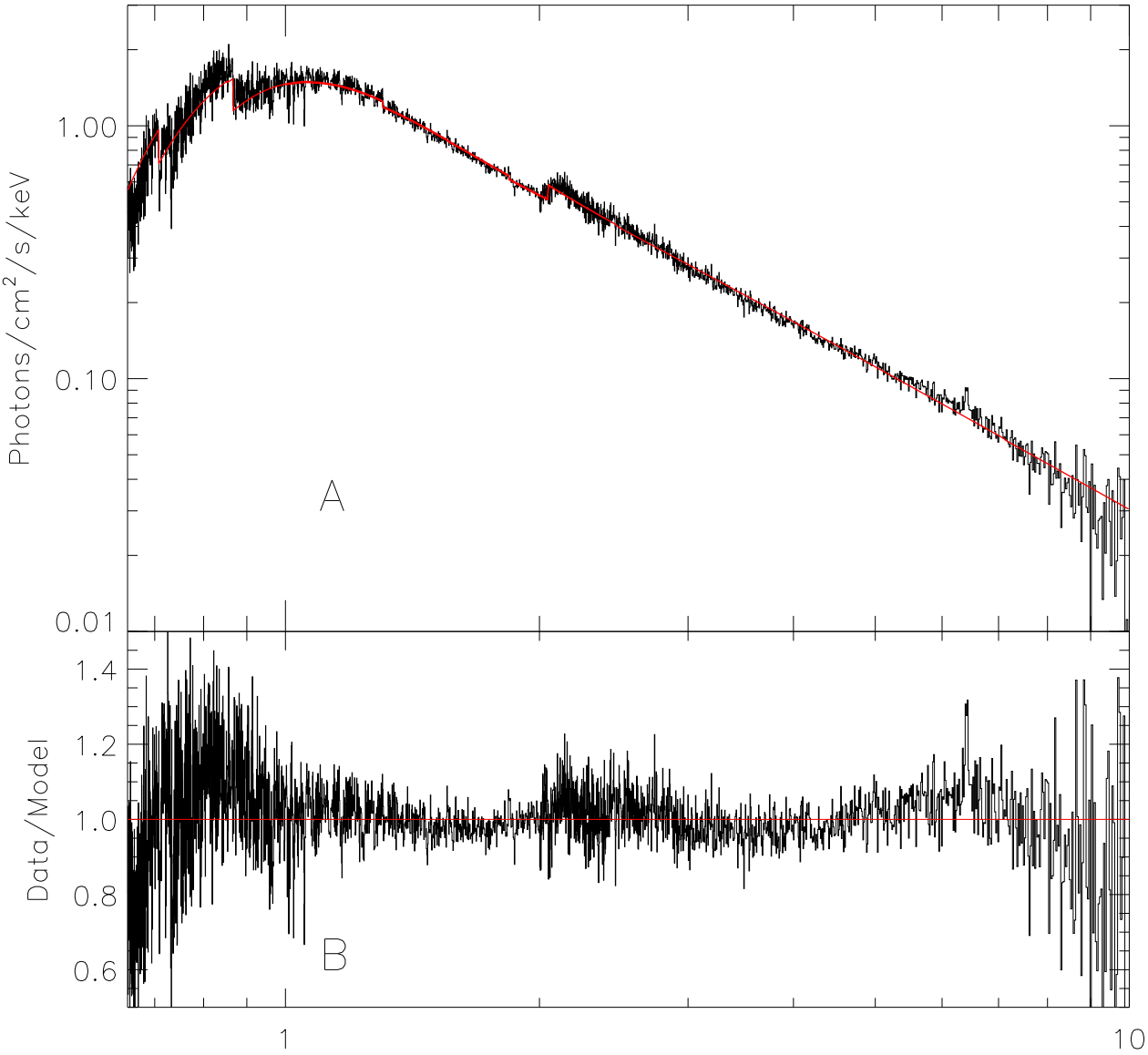

Fig. 2.— In panel A, the 0.65-10.0 keV spectrum is fit with a multicolor disk blackbody plus power-law continuum model (Model 1 in Table 1). The data/model ratio for this model is shown in panel B. We have suppressed a narrow instrumental feature at 1.85 keV. The notch at 2.05 keV is also an instrumental artifact. To portray the spectrum with greatest clarity, we have plotted the spectrum and ratio without errors. However, all errors are small compared to the deviations except below 0.7 keV and above 8.5 keV.

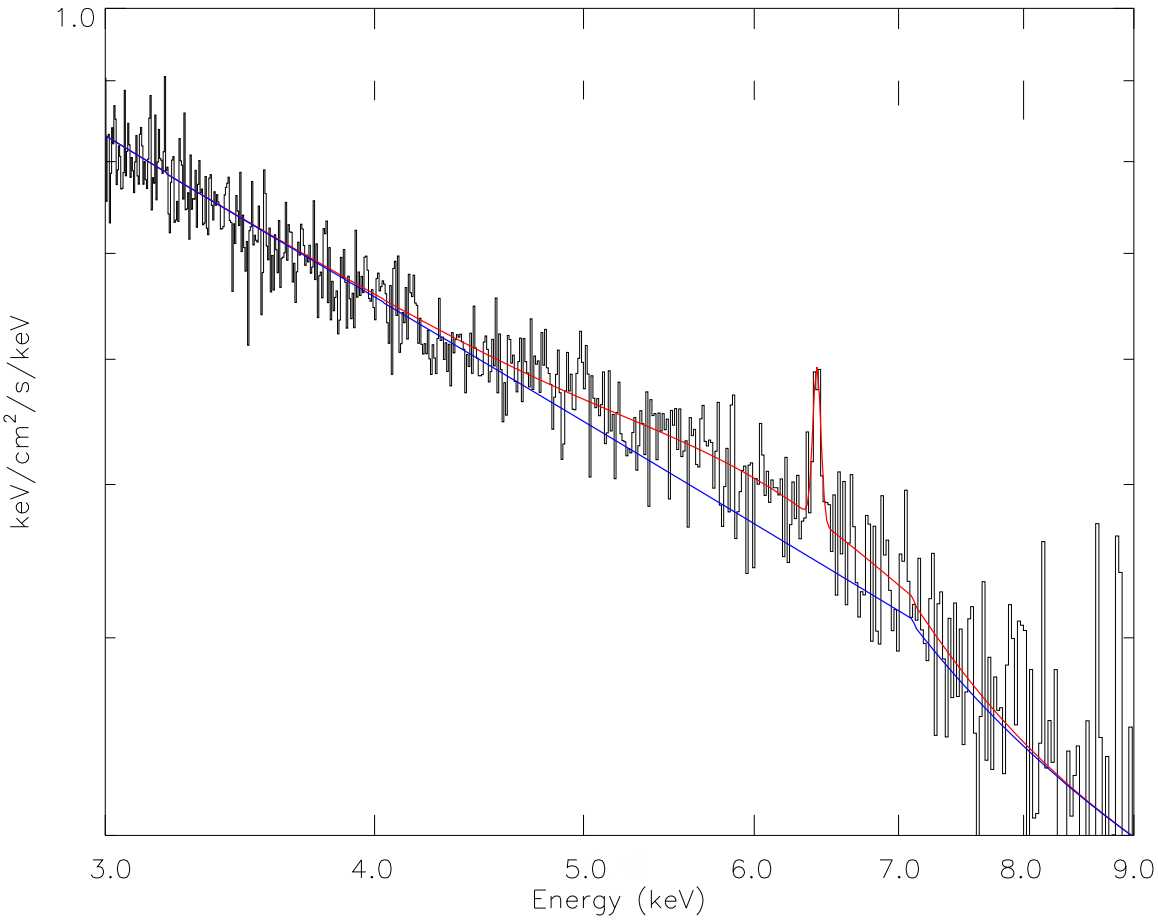

Fig. 3.— The HEG spectrum in the Fe Kα line region at full resolution. The fit in red corresponds to Model 3 in Table 1 (the continuum model is that of a multicolor disk blackbody plus a power-law). The fit includes broad and narrow Gaussian line components and a smeared Fe K edge. The continuum *not* including the lines is shown by the fit in blue. Representative error bars are indicated along the top of the plot. The resolution of the HEG reveals that the Fe Kα line in Cygnus X-1 is a composite of narrow and broad lines.

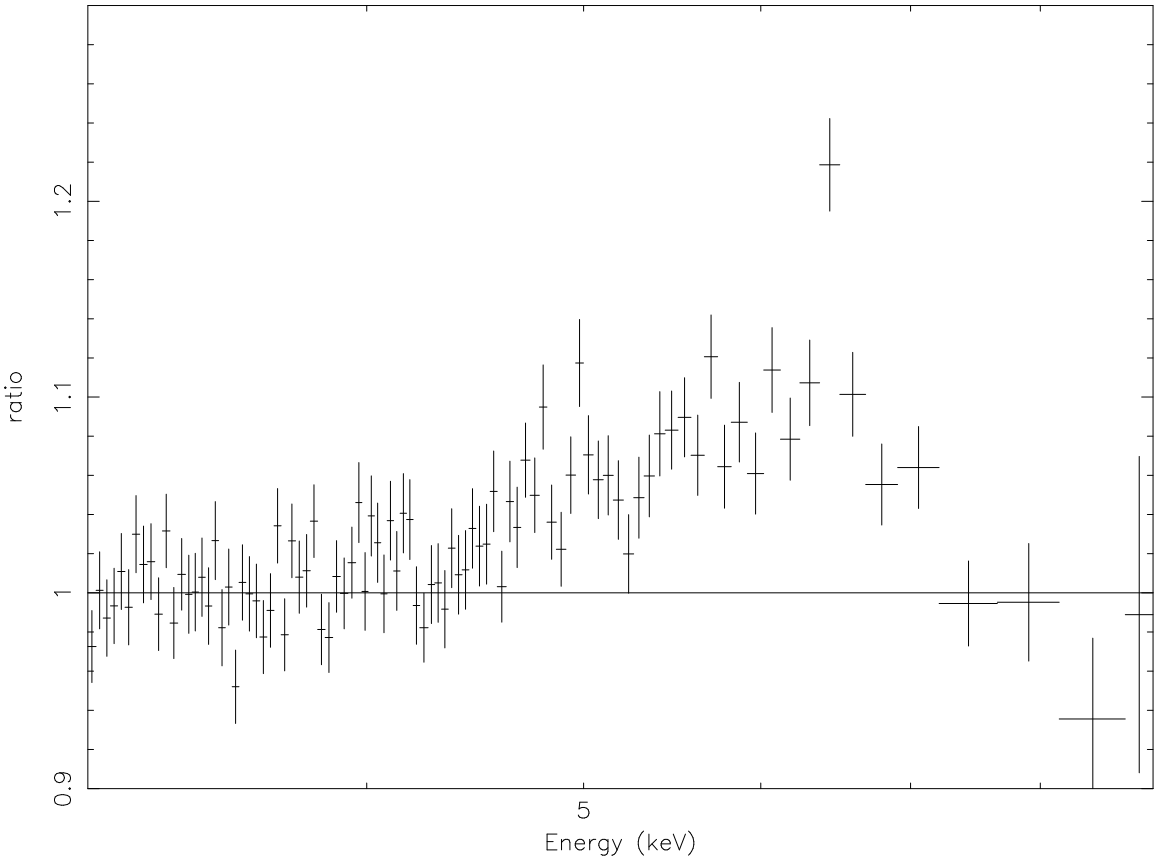

Fig. 4.— The data/model ratio of the Fe Kα line region, rebinned by a factor of 50 for visual clarity. The spectrum was fit with a simple multicolor disk blackbody plus power-law model (see Table 1), but ignoring the 4.0–7.2 keV region (following Iwasawa et al. 1996 for the Seyfert galaxy MCG –6–30–15). The data/model ratio above clearly displays an iron line profile which is very similar to profiles seen in active galactic nuclei.